# An improved interpolating element-free Galerkin method for elasticity*

Sun Feng-Xin(孙凤欣)[a)c)], Wang Ju-Feng(王聚丰)[a)b)], and Cheng Yu-Min(程玉民)[a)†]

[a)] *Shanghai Institute of Applied Mathematics and Mechanics, Shanghai Key Laboratory of Mechanics in Energy Engineering, Shanghai University, Shanghai* 200072, *China*

[b)] *Ningbo Institute of Technology, Zhejiang University, Ningbo* 315100, *China*

[c)] *Faculty of Science, Ningbo University of Technology, Ningbo* 315016, *China*

(Received 30 March 2013; revised manuscript received 2 May 2013)

Based on the improved interpolating moving least-squares (IIMLS) method and the Galerkin weak form, an improved interpolating element-free Galerkin (IIEFG) method is presented for two-dimensional elasticity problems in this paper. Compared with the interpolating moving least-squares (IMLS) method presented by Lancaster, the IIMLS method uses the nonsingular weight function. The number of unknown coefficients in the trial function of the IIMLS method is less than that of the MLS approximation and the shape function of the IIMLS method satisfies the property of Kronecker $\delta$ function. Thus in the IIEFG method, the essential boundary conditions can be applied directly and easily, then the numerical solutions can be obtained with higher precision than those obtained by the interpolating element-free Galerkin (IEFG) method. For the purposes of demonstration, four numerical examples are solved using the IIEFG method.

**Keywords:** meshless method, improved interpolating moving least-squares (IIMLS) method, improved interpolating element-free Galerkin (IIEFG) method, elasticity

**PACS:** 02.60.Cb, 02.60.Lj, 02.30.Em **DOI:** 10.1088/1674-1056/22/12/120203

## 1. Introduction

The finite element method (FEM)[1,2] and the boundary element method (BEM)[3] are very successful numerical methods for science and engineering problems. However, they cannot be effectively applied to some complicated problems, such as extremely large deformations and crack growth problems. In recent years, more and more attention has been paid to the research on the meshless (or meshfree) method. The most important common feature of meshless methods is that the trial function is constructed from a set of nodes with a minimum of meshing or no meshing at all. They show some advantages over FEM and BEM when solving the problems which are not well suited to traditional computational methods. Based on different approximation functions, many kinds of meshless methods have been proposed.[4–15]

The moving least-squares (MLS) approximation is one of the most widely used methods to form the shape function in the meshless method. The MLS approximation was introduced first by Shepard[16] for constructing smooth approximations to fit a specified cloud of points. It was then extended by Lancaster and Salkauskas[17] to surface generation problems. The shape function of the MLS approximation is simple, and the meshless method based on the MLS approximation can obtain a solution with high precision.[6–9]

The shape function of the MLS approximation does not satisfy the property of the Kronecker $\delta$ function. Then in meshless methods based on the MLS approximation, the essential boundary conditions cannot be applied directly.[7–9,15]

Lancaster and Salkauskas[17] presented an interpolating moving least-square (IMLS) method by using the singular weight function. The shape function of the IMLS method satisfies the property of the Kronecker $\delta$ function, and then the meshless methods based on the IMLS method can used as the essential boundary condition directly without any additional numerical effort. Kaljevic and Saigal[18] presented an improved formulation of the element-free Galerkin (EFG) method based on the IMLS method. Ren *et al.*[19–22] revised the formulae of the IMLS method, and presented an interpolating element-free Galerkin (IEFG) method and an interpolating boundary element-free (IBEF) method for potential and elasticity problems. In the IEFG and IBEF methods, the essential boundary conditions are applied directly.

A disadvantage of the IMLS method is that the weight function used in it must be singular at nodes. The singular weight function makes the matrix in the system equation singular, which causes many difficulties in obtaining the derivatives of the approximation function in the IMLS method. To be free from the requirement of the singularity, Netuzhylov[23] presented the perturbation technique in the IMLS method by using a small positive number $\varepsilon$ within the regularized weight function matrix. Thomas and Christian[24] also presented a special non-singular interpolating weighting function, then the

*Project supported by the National Natural Science Foundation of China (Grant No. 11171208) and the Shanghai Leading Academic Discipline Project, China (Grant No. S30106).

†Corresponding author. E-mail: ymcheng@shu.edu.cn

© 2013 Chinese Physical Society and IOP Publishing Ltd 

MLS shape functions satisfy the interpolation condition exactly.

To be free from the requirement of the singularity, Wang *et al.*[25] presented an improved interpolating moving least-squares (IIMLS) method. The shape function of the IIMLS method satisfies the property of the Kronecker $\delta$ function. Thus the essential boundary condition can be applied directly and easily in meshless methods based on the IIMLS method. Compared with the IMLS method presented by Lancaster and Salkauskas, the weight function used in the IIMLS method is not singular at any point. Any weight function used in the MLS approximation can be applied in the IIMLS method. Then the IIMLS method can overcome the difficulties caused by the singular weight function in the IMLS method. And the number of the unknown coefficients in the trial function of the IIMLS method is less than that of the MLS approximation. Then we can select fewer nodes in the local influence domain in the IIMLS method, and high computational precision can be obtained.

In this paper, combining the IIMLS method with the Galerkin weak form of elasticity problems, an improved interpolating element-free Galerkin (IIEFG) method is presented for two-dimensional elasticity problems. In the IIEFG method, the essential boundary conditions are applied naturally and directly. Thus the IIEFG method gives a high computational precision. For the purposes of demonstration, some selected numerical examples are solved using the IIEFG method.

## 2. Improved interpolating moving least-squares method

Let $p_1(\boldsymbol{x}), p_2(\boldsymbol{x}), \ldots, p_m(\boldsymbol{x})$ be the given basis functions, and $p_1(\boldsymbol{x}) \equiv 1$. In order to let the shape function of the IIMLS method, in which the nonsingular weight function is used, satisfy the property of the Kronecker $\delta$ function, we first generate a new set of basis functions.

For a given point $\boldsymbol{x} \in \Omega$, let

$$\tilde{p}_i(\bar{\boldsymbol{x}})_x = p_i(\bar{\boldsymbol{x}}) - \sum_{I=1}^{n} v(\boldsymbol{x}, \boldsymbol{x}_I) p_i(\boldsymbol{x}_I), \quad i = 1,2,\ldots,m, \tag{1}$$

where $\bar{\boldsymbol{x}}$ is the point in the local approximation of $\boldsymbol{x}$, $\boldsymbol{x}_I$ $(I = 1,2,\ldots,n)$ are the nodes with domains of influence that cover the point $\boldsymbol{x}$, and

$$v(\boldsymbol{x}, \boldsymbol{x}_I) = \frac{\zeta(\boldsymbol{x}, \boldsymbol{x}_I)}{\sum\limits_{J=1}^{n} \zeta(\boldsymbol{x}, \boldsymbol{x}_J)}, \tag{2}$$

$$\zeta(\boldsymbol{x}, \boldsymbol{x}_I) = \frac{\prod\limits_{J \neq I} ||\boldsymbol{x} - \boldsymbol{x}_J||^2}{\prod\limits_{J \neq I} ||\boldsymbol{x}_I - \boldsymbol{x}_J||^2}. \tag{3}$$

Applying the same transformation to $u(\boldsymbol{x})$, we have

$$\tilde{u}(\bar{\boldsymbol{x}})_x = u(\bar{\boldsymbol{x}}) - \sum_{I=1}^{n} v(\boldsymbol{x}, \boldsymbol{x}_I) u(\boldsymbol{x}_I). \tag{4}$$

The function $v(\boldsymbol{x}, \boldsymbol{x}_I)$ obviously satisfies

$$v(\boldsymbol{x}_I, \boldsymbol{x}_J) = \delta_{IJ}, \tag{5}$$

and

$$\sum_{I=1}^{n} v(\boldsymbol{x}, \boldsymbol{x}_I) = 1, \ \ \forall x \in \Omega. \tag{6}$$

Next, we will obtain the approximation function of the new function $\tilde{u}(\bar{\boldsymbol{x}})_x$ by the MLS approximation with the new basis functions.

Define a local approximation function as

$$\tilde{u}_L(\boldsymbol{x}, \bar{\boldsymbol{x}}) = \sum_{i=1}^{m} \tilde{p}_i(\bar{\boldsymbol{x}})_x \tilde{\boldsymbol{a}}_i(\boldsymbol{x}), \tag{7}$$

where $\tilde{\boldsymbol{a}}_i(\boldsymbol{x})$ are the unknown coefficients of the new basis.

From Eqs. (1) and (6), we have

$$\tilde{p}_1(\bar{\boldsymbol{x}})_x = 1 - \sum_{I=1}^{n} v(\boldsymbol{x}, \boldsymbol{x}_I) = 0. \tag{8}$$

Then

$$\tilde{u}_L(\boldsymbol{x}, \bar{\boldsymbol{x}}) = \sum_{i=2}^{m} \tilde{p}_i(\bar{\boldsymbol{x}})_x \tilde{\boldsymbol{a}}_i(\boldsymbol{x}). \tag{9}$$

The $m-1$ coefficients $\tilde{\boldsymbol{a}}_i(\boldsymbol{x})$, $i = 2,3,\ldots,m$, can be obtained by using the weighted least-square method.

Define a functional

$$\begin{aligned} \tilde{J} &= \sum_{I=1}^{n} w(\boldsymbol{x} - \boldsymbol{x}_I)[\tilde{u}_L(\boldsymbol{x}, \boldsymbol{x}_I) - \tilde{u}(\boldsymbol{x}_I)_x]^2 \\ &= \sum_{I=1}^{n} w(\boldsymbol{x} - \boldsymbol{x}_I) \Bigg[ \sum_{I=1}^{n} v(\boldsymbol{x}, \boldsymbol{x}_I) u(\boldsymbol{x}_I) \\ &\quad + \sum_{i=2}^{m} \tilde{p}_i(\boldsymbol{x}_I)_x \tilde{\boldsymbol{a}}_i(\boldsymbol{x}) - u(\boldsymbol{x}_I) \Bigg]^2, \end{aligned} \tag{10}$$

then equation (10) can be written as

$$\begin{aligned} \tilde{J} &= (\boldsymbol{V}(\boldsymbol{x})\boldsymbol{u} + \tilde{\boldsymbol{P}}(\boldsymbol{x})\tilde{\boldsymbol{a}}(\boldsymbol{x}) - \boldsymbol{u})^{\mathrm{T}} \boldsymbol{W}(\boldsymbol{x}) (\boldsymbol{V}(\boldsymbol{x})\boldsymbol{u} \\ &\quad + \tilde{\boldsymbol{P}}(\boldsymbol{x})\tilde{\boldsymbol{a}}(\boldsymbol{x}) - \boldsymbol{u}), \end{aligned} \tag{11}$$

where

$$\tilde{\boldsymbol{a}}^{\mathrm{T}}(\boldsymbol{x}) = (\tilde{\boldsymbol{a}}_2(\boldsymbol{x}), \tilde{\boldsymbol{a}}_3(\boldsymbol{x}), \ldots, \tilde{\boldsymbol{a}}_m(\boldsymbol{x})), \tag{12}$$

$$\boldsymbol{u}^{\mathrm{T}} = (u(\boldsymbol{x}_1), u(\boldsymbol{x}_2), \ldots, u(\boldsymbol{x}_n)), \tag{13}$$

$$\boldsymbol{W}(\boldsymbol{x}) = \begin{bmatrix} w(\boldsymbol{x} - \boldsymbol{x}_1) & 0 & \cdots & 0 \\ 0 & w(\boldsymbol{x} - \boldsymbol{x}_2) & \cdots & 0 \\ \vdots & \vdots & \ddots & \vdots \\ 0 & 0 & \cdots & w(\boldsymbol{x} - \boldsymbol{x}_n) \end{bmatrix}, \tag{14}$$

$$\tilde{\boldsymbol{P}}(\boldsymbol{x}) = \begin{bmatrix} \tilde{p}_2(\boldsymbol{x}_1)_x & \tilde{p}_3(\boldsymbol{x}_1)_x & \cdots & \tilde{p}_m(\boldsymbol{x}_1)_x \\ \tilde{p}_2(\boldsymbol{x}_2)_x & \tilde{p}_3(\boldsymbol{x}_2)_x & \cdots & \tilde{p}_m(\boldsymbol{x}_2)_x \\ \vdots & \vdots & \ddots & \vdots \\ \tilde{p}_2(\boldsymbol{x}_n)_x & \tilde{p}_3(\boldsymbol{x}_n)_x & \cdots & \tilde{p}_m(\boldsymbol{x}_n)_x \end{bmatrix}, \tag{15}$$

and $\boldsymbol{V}(\boldsymbol{x})$ is an $n \times n$ matrix in which each row is

$$\boldsymbol{v}(\boldsymbol{x}) = (v(\boldsymbol{x}, \boldsymbol{x}_1), v(\boldsymbol{x}, \boldsymbol{x}_2), \ldots, v(\boldsymbol{x}, \boldsymbol{x}_n)). \tag{16}$$

To obtain $\tilde{\boldsymbol{a}}_i(\boldsymbol{x})$, we let

$$\frac{\partial \tilde{J}}{\partial \tilde{\boldsymbol{a}}} = \tilde{\boldsymbol{A}}(x)\tilde{\boldsymbol{a}}(\boldsymbol{x}) - \tilde{\boldsymbol{B}}(\boldsymbol{x})\boldsymbol{u} = 0, \tag{17}$$

where

$$\tilde{\boldsymbol{A}}(\boldsymbol{x}) = \tilde{\boldsymbol{P}}^{\mathrm{T}}(\boldsymbol{x})\boldsymbol{W}(\boldsymbol{x})\tilde{\boldsymbol{P}}(\boldsymbol{x}), \tag{18}$$

$$\tilde{\boldsymbol{B}}(\boldsymbol{x}) = \tilde{\boldsymbol{P}}^{\mathrm{T}}(\boldsymbol{x})\boldsymbol{W}(\boldsymbol{x})(\boldsymbol{E} - \boldsymbol{V}(\boldsymbol{x})), \tag{19}$$

and $\boldsymbol{E}$ is an $n \times n$ identity matrix.

From Eq. (17) we have

$$\tilde{\boldsymbol{a}}(\boldsymbol{x}) = \tilde{\boldsymbol{A}}^{-1}(\boldsymbol{x})\tilde{\boldsymbol{B}}(\boldsymbol{x})\boldsymbol{u}. \tag{20}$$

Then the local approximation function can be obtained as

$$\tilde{u}_L(\boldsymbol{x}, \bar{\boldsymbol{x}}) = \sum_{i=2}^{m} \tilde{p}_i(\bar{\boldsymbol{x}})_x \tilde{\boldsymbol{a}}_i(\boldsymbol{x}) = \hat{\boldsymbol{p}}(\bar{\boldsymbol{x}})_x \tilde{\boldsymbol{A}}^{-1}(\boldsymbol{x})\tilde{\boldsymbol{B}}(\boldsymbol{x})\boldsymbol{u}, \tag{21}$$

where

$$\hat{\boldsymbol{p}}(\bar{\boldsymbol{x}})_x = (\tilde{p}_2(\bar{\boldsymbol{x}})_x, \tilde{p}_3(\bar{\boldsymbol{x}})_x, \ldots, \tilde{p}_m(\bar{\boldsymbol{x}})_x). \tag{22}$$

From Eqs. (4) and (21), the global interpolating approximation function of $u(\boldsymbol{x})$ is obtained as

$$u^h(\boldsymbol{x}) = \tilde{\boldsymbol{\Phi}}(\boldsymbol{x})\boldsymbol{u} = \sum_{I=1}^{n} \tilde{\Phi}_I(\boldsymbol{x})u(\boldsymbol{x}_I), \tag{23}$$

where $\tilde{\boldsymbol{\Phi}}(x)$ is the shape function vector,

$$\begin{aligned} \tilde{\boldsymbol{\Phi}}(\boldsymbol{x}) &= (\tilde{\Phi}_1(\boldsymbol{x}), \tilde{\Phi}_2(\boldsymbol{x}), \ldots, \tilde{\Phi}_n(\boldsymbol{x})) \\ &= \boldsymbol{v}(\boldsymbol{x}) + \tilde{\boldsymbol{p}}^{\mathrm{T}}(\boldsymbol{x})\tilde{\boldsymbol{A}}^{-1}(\boldsymbol{x})\tilde{\boldsymbol{B}}(\boldsymbol{x}), \end{aligned} \tag{24}$$

and

$$\tilde{\boldsymbol{p}}^{\mathrm{T}}(\boldsymbol{x}) = (g_2(\boldsymbol{x}), g_3(\boldsymbol{x}), \ldots, g_m(\boldsymbol{x})), \tag{25}$$

$$g_i(\boldsymbol{x}) = p_i(\boldsymbol{x}) - \sum_{I=1}^{n} v(\boldsymbol{x}, \boldsymbol{x}_I)p_i(\boldsymbol{x}_I). \tag{26}$$

Equation (24) is the shape function of the IIMLS method, and then the IIMLS method is presented.

The shape function of the IIMLS method can satisfy the property of the Kronecker $\delta$ function. Compared with the IMLS method presented by Lancaster and Salkauskas, the nonsingular weight function is used in the IIMLS method. Then any weight function used in the MLS approximation can also be applied in the IIMLS method.

From Eq. (9), it can be seen that the number of the unknown coefficients in the trial function of the IIMLS method is less than that in the trial function of the MLS approximation. Therefore we can select fewer nodes in the meshless method based on the IIMLS method than those based on the MLS approximation.

## 3. The improved interpolating element-free Galerkin method for elasticity

Based on the IIMLS method and the Galerkin weak form, an interpolating element-free Galerkin (IIEFG) method is proposed for two-dimensional linear elasticity problems.

We employ $n_t$ nodes in the domain $\Omega$, and the union of its compact support domains must cover the whole domain $\Omega$. For elasticity problems, from the IIMLS method, the displacement at an arbitrary point $x$ in the domain can be expressed as

$$\boldsymbol{u}(\boldsymbol{x}) = (u_1(\boldsymbol{x}), u_2(\boldsymbol{x}))^{\mathrm{T}}, \tag{27}$$

and

$$u_1(\boldsymbol{x}) = \sum_{I=1}^{n} \tilde{\Phi}_I(\boldsymbol{x})u_1(\boldsymbol{x}_I), \tag{28}$$

$$u_2(\boldsymbol{x}) = \sum_{I=1}^{n} \tilde{\Phi}_I(\boldsymbol{x})u_2(\boldsymbol{x}_I), \tag{29}$$

where $n$ is the number of nodes whose compact support domains cover the point $\boldsymbol{x}$.

Then it follows from Eq. (27) that

$$\boldsymbol{u} = \boldsymbol{N}(\boldsymbol{x})\boldsymbol{U}, \tag{30}$$

where

$$\begin{aligned} \boldsymbol{U} = (&u_1(\boldsymbol{x}_1), u_2(\boldsymbol{x}_1), u_1(\boldsymbol{x}_2), u_2(\boldsymbol{x}_2), \ldots, \\ &u_1(\boldsymbol{x}_n), u_2(\boldsymbol{x}_n))^{\mathrm{T}}, \end{aligned} \tag{31}$$

$$\boldsymbol{N}(\boldsymbol{x}) = (N_1(\boldsymbol{x}), N_2(\boldsymbol{x}), \ldots, N_n(\boldsymbol{x})), \tag{32}$$

$$\boldsymbol{N}_I(\boldsymbol{x}) = \begin{bmatrix} \tilde{\Phi}_I(\boldsymbol{x}) & 0 \\ 0 & \tilde{\Phi}_I(\boldsymbol{x}) \end{bmatrix}. \tag{33}$$

The strain can be expressed as

$$\begin{aligned} \boldsymbol{\varepsilon}(\boldsymbol{x}) &= \begin{bmatrix} u_{1,1} \\ u_{2,2} \\ u_{1,2} + u_{2,1} \end{bmatrix} \\ &= \begin{bmatrix} \sum\limits_{I=1}^{n} \tilde{\Phi}_{I,1}(\boldsymbol{x})u_1(\boldsymbol{x}_I) \\ \sum\limits_{I=1}^{n} \tilde{\Phi}_{I,2}(\boldsymbol{x})u_2(\boldsymbol{x}_I) \\ \sum\limits_{I=1}^{n} \tilde{\Phi}_{I,2}(\boldsymbol{x})u_1(\boldsymbol{x}_I) + \sum\limits_{I=1}^{n} \tilde{\Phi}_{I,1}(\boldsymbol{x})u_2(\boldsymbol{x}_I) \end{bmatrix} \\ &\equiv \boldsymbol{B}(\boldsymbol{x})\boldsymbol{U}, \end{aligned} \tag{34}$$

where

$$\boldsymbol{B}(\boldsymbol{x}) = (\boldsymbol{B}_1(\boldsymbol{x}), \boldsymbol{B}_2(\boldsymbol{x}), \ldots, \boldsymbol{B}_n(\boldsymbol{x})), \tag{35}$$

$$\boldsymbol{B}_I(\boldsymbol{x}) = \begin{bmatrix} \tilde{\Phi}_{I,1}(\boldsymbol{x}) & 0 \\ 0 & \tilde{\Phi}_{I,2}(\boldsymbol{x}) \\ \tilde{\Phi}_{I,2}(\boldsymbol{x}) & \tilde{\Phi}_{I,1}(\boldsymbol{x}) \end{bmatrix}. \tag{36}$$

Then the stress-strain relation is

$$\boldsymbol{\sigma}(\boldsymbol{x}) = \boldsymbol{D} \cdot \boldsymbol{\varepsilon}(\boldsymbol{x}) = \boldsymbol{D}\boldsymbol{B}(\boldsymbol{x})\boldsymbol{U}, \tag{37}$$

where

$$\boldsymbol{D} = \frac{E}{1-\nu^2}\begin{bmatrix} 1 & \nu & 0 \\ \nu & 1 & 0 \\ 0 & 0 & (1-\nu)/2 \end{bmatrix} \tag{38}$$

for a plane stress problem, and

$$\boldsymbol{D} = \frac{E}{(1+\nu)(1-2\nu)}\begin{bmatrix} 1-\nu & \nu & 0 \\ \nu & 1-\nu & 0 \\ 0 & 0 & (1-2\nu)/2 \end{bmatrix} \tag{39}$$

for a plane strain problem, $E$ is the Young's modulus and $\nu$ is the Poisson's ratio.

We consider the following two-dimensional problem on the domain $\Omega$ bounded by $\Gamma$:

$$\nabla \cdot \boldsymbol{\sigma} + \boldsymbol{b} = 0, \ \text{in} \ \Omega, \tag{40}$$

where $\boldsymbol{\sigma}$ is the stress tensor and $\boldsymbol{b}$ is the body force vector.

The corresponding boundary conditions are

$$\boldsymbol{u} = \boldsymbol{u}_0, \ \text{on} \ \Gamma_u, \tag{41}$$

$$\boldsymbol{t} = \boldsymbol{\sigma} \cdot \boldsymbol{n} = \boldsymbol{t}_0, \ \text{on} \ \Gamma_\sigma, \tag{42}$$

where $\boldsymbol{t}$ is the traction vector, $\boldsymbol{u}_0$ and $\boldsymbol{t}_0$ are respectively the prescribed displacement and traction vector on the displacement boundary $\Gamma_u$ and on the traction boundary $\Gamma_\sigma$, and $\boldsymbol{n}$ is the unit outward normal to the boundary $\Gamma$.

The Galerkin weak form of Eqs. (40)–(42) is

$$\int_\Omega \boldsymbol{\sigma}^{\mathrm{T}} \delta\boldsymbol{\varepsilon} \mathrm{d}\Omega - \int_\Omega \boldsymbol{b}^{\mathrm{T}} \delta\boldsymbol{u} \mathrm{d}\Omega - \int_{\Gamma_\sigma} \boldsymbol{t}^{\mathrm{T}} \delta\boldsymbol{u} \mathrm{d}\Gamma = 0, \tag{43}$$

where $\delta$ is the variational operator.

Substituting Eqs. (30), (34), and (37) into Eq. (43) yields

$$\int_\Omega (\boldsymbol{DB}(\boldsymbol{x})\boldsymbol{U})^{\mathrm{T}} \delta(\boldsymbol{B}(\boldsymbol{x})\boldsymbol{U}) \mathrm{d}\Omega - \int_\Omega \boldsymbol{b}^{\mathrm{T}} \delta(\boldsymbol{N}(\boldsymbol{x})\boldsymbol{U}) \mathrm{d}\Omega - \int_{\Gamma_\sigma} \boldsymbol{t}^{\mathrm{T}} \delta(\boldsymbol{N}(\boldsymbol{x})\boldsymbol{U}) \mathrm{d}\Gamma = 0, \tag{44}$$

i.e.,

$$(\delta\boldsymbol{U})^{\mathrm{T}} \left[ \int_\Omega \boldsymbol{B}^{\mathrm{T}}(\boldsymbol{x}) \boldsymbol{DB}(\boldsymbol{x}) \boldsymbol{U} \mathrm{d}\Omega - \int_\Omega \boldsymbol{N}^{\mathrm{T}}(\boldsymbol{x}) \boldsymbol{b} \mathrm{d}\Omega - \int_{\Gamma_\sigma} \boldsymbol{N}^{\mathrm{T}}(\boldsymbol{x}) \boldsymbol{t} \mathrm{d}\Gamma \right] = 0. \tag{45}$$

Because the nodal test function $\delta\boldsymbol{U}$ is arbitrary, the final discretized equation is obtained as

$$\boldsymbol{KU} = \boldsymbol{f}, \tag{46}$$

where

$$\boldsymbol{K}_{IJ} = \int_\Omega \boldsymbol{B}_I^{\mathrm{T}} \boldsymbol{DB}_J \mathrm{d}\Omega, \tag{47}$$

$$\boldsymbol{f}_I = \int_\Omega \boldsymbol{N}_I^{\mathrm{T}} \boldsymbol{b} \mathrm{d}\Omega + \int_{\Gamma_t} \boldsymbol{N}_I^{\mathrm{T}} \boldsymbol{t} \mathrm{d}\Gamma. \tag{48}$$

Since the shape function of the IIMLS method satisfies the property of the Kronecker $\delta$ function, the essential boundary conditions can be applied directly. And then, substituting the boundary conditions of Eq. (41) into Eq. (46), we can obtain the unknowns at nodes by solving the linear equations (46).

Thus the IIEFG method is presented for two-dimensional elasticity problems.

## 4. Numerical examples

Four example problems are presented to demonstrate the applicability of the IIEFG method for two-dimensional elasticity problems. The linear basis function and the cubic spline weight function are used in these examples. The results of the IIEFG method are compared with the existing analytical results and the ones of the IEFG method or ABAQUS software.

The first example considered is a Timoshenko beam subjected to a parabolic traction at the free end as shown in Fig. 1. The beam is of length $L$ and height $D$, and has a unit thickness. The beam is assumed to be in a state of plane stress. This is a benchmark problem and the corresponding analytical solution is available.[26]

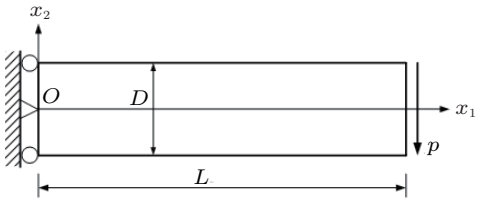



**Fig. 1.** Cantilever beam.

The problem is solved with $E = 3.0 \times 10^7$ Pa, $\nu = 0.3$, $L = 48$ m, $D = 12$ m, and $p = 1000$ N.

Regular nodal distribution as shown in Fig. 2 is employed. To evaluate the stiffness matrix, $20 \times 8$ background integration cell structure is used, and $4 \times 4$ Gauss quadrature is employed in each integration cell.

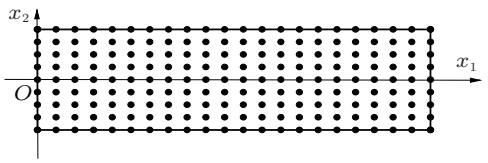



**Fig. 2.** Node distribution of the cantilever beam.

The numerical solutions of the deflection of the beam along the $x_1$ axis by the IIEFG and IEFG methods are shown in Fig. 3. It is evident that the numerical results of this paper are in excellent agreement with the analytical results. The stresses $\sigma_{11}$ and $\sigma_{12}$ using the IIEFG and IEFG methods at the section of $x_1 = L/2$ are shown in Figs. 4 and 5. The results of

this paper also accord well with the analytical results and the IIEFG method has higher accuracy than the IEFG method.

For the error analysis, define the following energy norm:

$$e_\varepsilon = \sqrt{\frac{1}{2}\int_\Omega (\varepsilon^{\text{num}} - \varepsilon^{\text{exact}})^{\text{T}} D(\varepsilon^{\text{num}} - \varepsilon^{\text{exact}})\,\mathrm{d}\Omega}, \quad (49)$$

where $\varepsilon^{\text{num}}$ and $\varepsilon^{\text{exact}}$ are respectively the numerical and analytical solutions of the strain tensor.

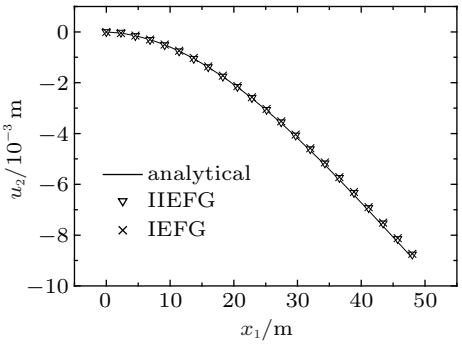



**Fig. 3.** Displacement $u_2$ along the $x_1$ axis.

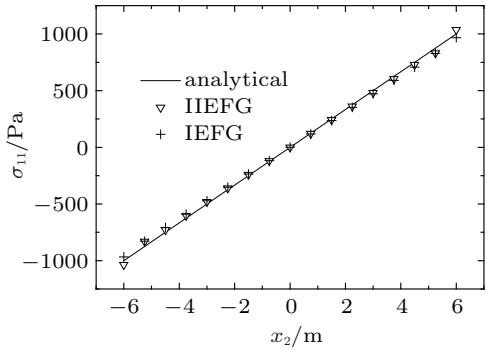



**Fig. 4.** Stress $\sigma_{11}$ at $x_1 = L/2$.

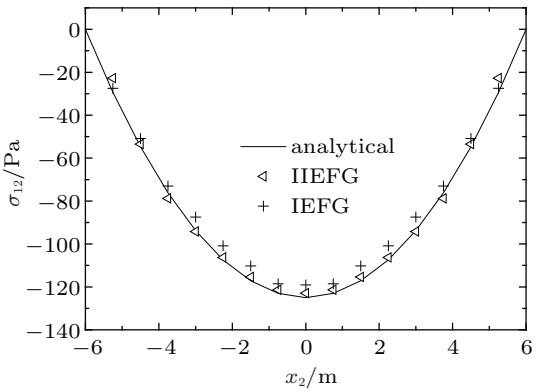



**Fig. 5.** Stress $\sigma_{12}$ at $x_1 = L/2$.

To study the convergence, the regular $13 \times 7$, $17 \times 9$, $21 \times 11$, and $25 \times 13$ nodes are employed. Then the rates of convergence in energy norm for this problem using the IIEFG and IEFG methods are shown in Fig. 6. The value $h$ is chosen to be the horizontal distance between the nodes in the model, and in each case $d_{\max} = 2$. The present results show that the convergence of the IIEFG method is good.

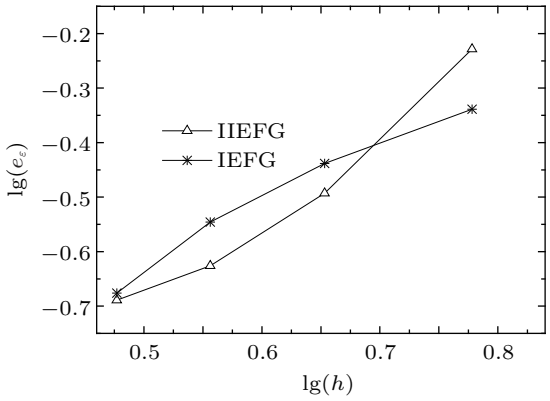



**Fig. 6.** Convergence of energy error norm.

The second example is a perforated plate with a central circular hole as shown in Fig. 7. The plate is subjected to a distributed load $p = 1000$ N/m in the $x_1$-axis direction. Suppose that the plate is in the plane stress state, and $\nu = 0.25$, $E = 2.0 \times 10^7$ Pa. When the condition $b/a \geq 5$ is satisfied, the solution of this finite plate is very close to that of the infinite plate. The analytical solution of an infinite plate is available.[26]

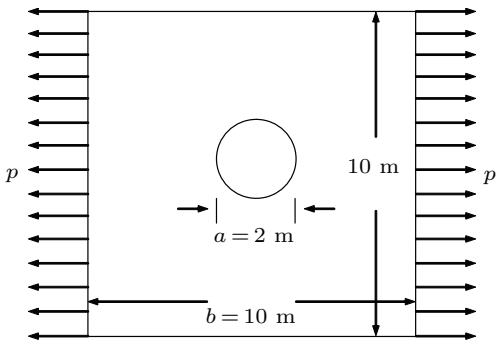



**Fig. 7.** A rectangular plate with a hole under a distributed load.

Due to the symmetry of the model, only a quarter of the model needs to be considered in the analysis (see Fig. 8). The nodal distribution shown in Fig. 9 is employed.

The values of displacement $u_r$ at $\theta = 0$ and $\pi/2$ by the IIEFG and IEFG methods are respectively shown in Figs. 10 and 11. And the stresses $\sigma_\theta$ at $\theta = \pi/2$ are shown in Fig. 12. Again, the IIEFG method has higher accuracy than the IEFG method.

The third example considered is a circular ring with the radii $b = 5$ m and $a = 1$ m (see Fig. 13). The distributed inner pressure is $p = 1000$ N/m. The ring is in the plane stress state, and $\nu = 0.25$, $E = 10^6$ Pa.

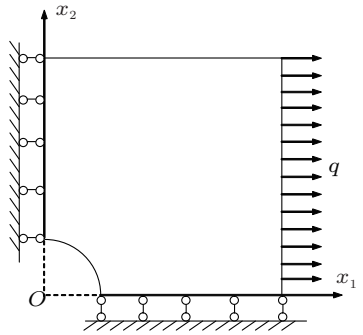



**Fig. 8.** A quarter of the rectangular plate and the boundary conditions.

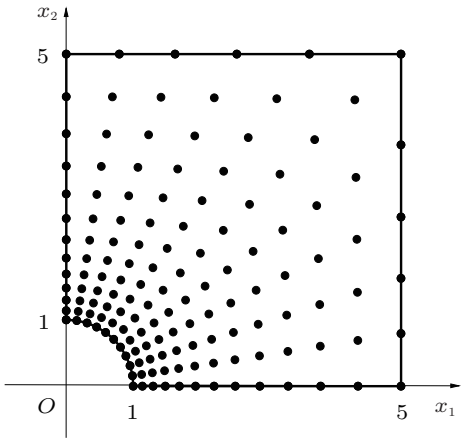



**Fig. 9.** The nodes in the domain of the rectangular plate with a hole.

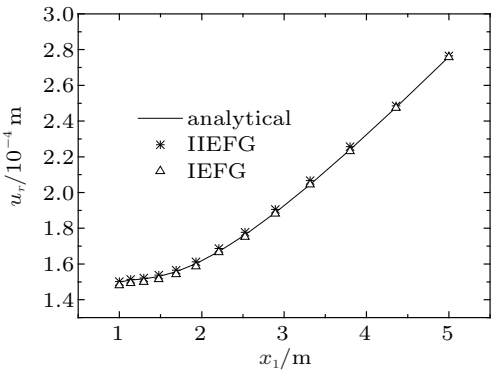



**Fig. 10.** Displacement $u_r$ at $\theta = 0$.

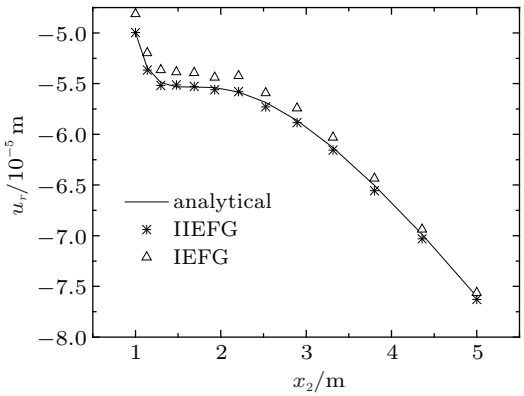



**Fig. 11.** Displacement $u_r$ at $\theta = \pi/2$.

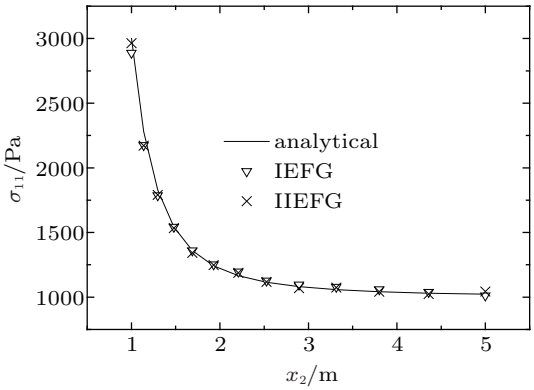



**Fig. 12.** Stress $\sigma_{11}$ at $\theta = \pi/2$.

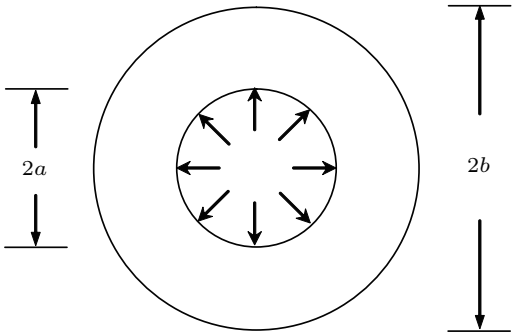



**Fig. 13.** A circular ring under a distributed inner pressure.

Due to the symmetry, only a quarter of the model needs to be considered (see Fig. 14), and the node distribution shown in Fig. 15 is used.

The values of displacement $u_r$ at $\theta = 0$ by the IIEFG and IEFG methods are all shown in Fig. 16. And the values of stress $\sigma_\theta$ at $\theta = 0$ are shown in Fig. 17. It can also be seen that the results obtained using the IIEFG method show excellent agreement with the analytical results.

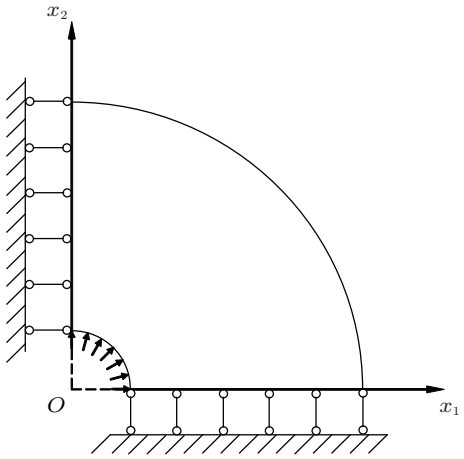



**Fig. 14.** The numerical model of the circular ring.

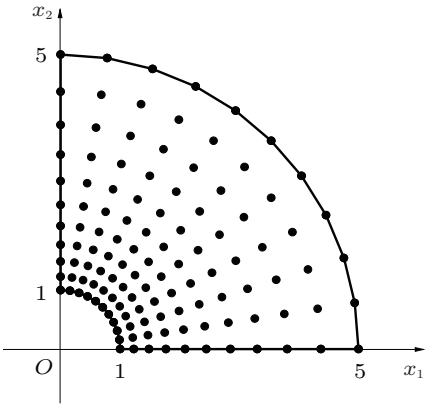



**Fig. 15.** Node distribution.

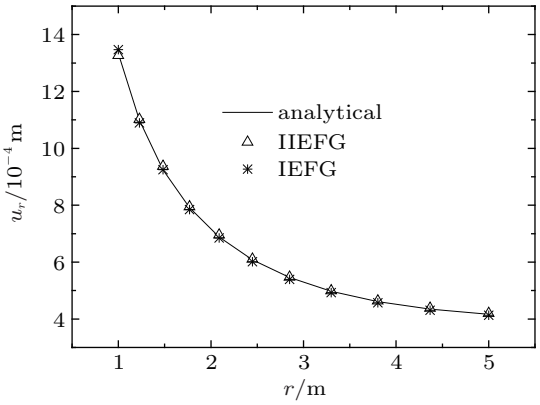



**Fig. 16.** Displacement $u_r$ at $\theta = 0$.

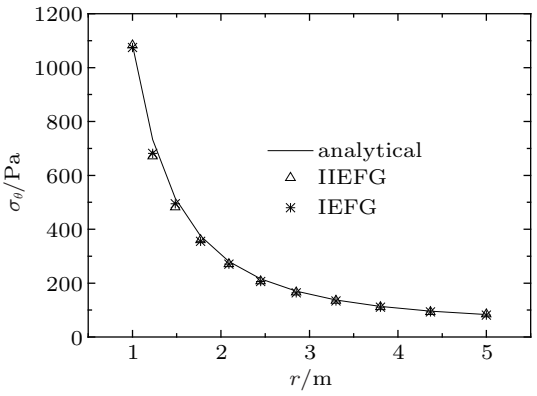



**Fig. 17.** Stress $\sigma_\theta$ at $\theta = 0$.

The fourth example considered is a bridge pier as shown in Fig. 18.[27] Suppose that it is subjected to a distributed load $p = 50$ kN/m on the top of the pier. The bridge is in the plane strain state with $\nu = 0.15$, $E = 40$ GPa. Considering the symmetry of the bridge, only the right half of the pier is modeled as shown in Fig. 19.

The node arrangement used by the IIEFG method is shown in Fig. 19. The problem is also analyzed by FEM software ABAQUS. The displacements of the IIEFG method and ABAQUS on boundary curves *EAB* are shown in Fig. 20. The results obtained by the present method are in very good agreement with those obtained by using ABAQUS.

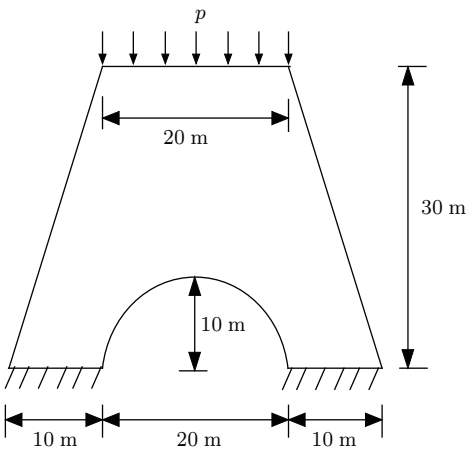



**Fig. 18.** A bridge pier.

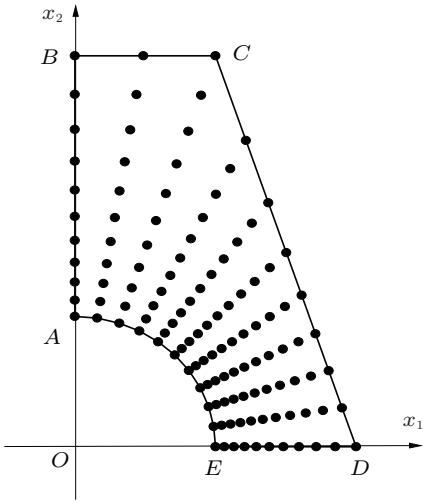



**Fig. 19.** Node distribution.

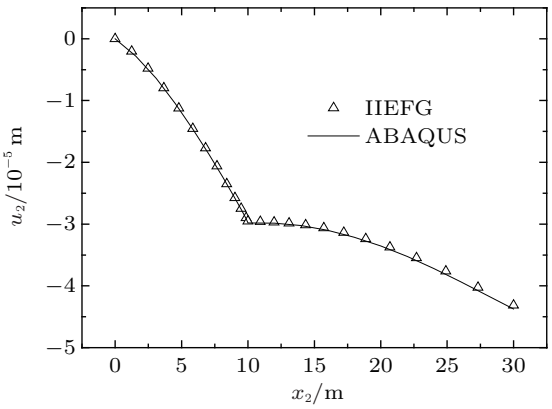



**Fig. 20.** Displacement $u_2$ on curve *EAB*.

## 5. Conclusions

Based on the IIMLS method and the Galerkin weak form, the IIEFG method for two-dimensional plasticity problems is presented in this paper. The shape function of the IIMLS method satisfies the property of the Kronecker $\delta$ function.

Then in the IIEFG method, the essential boundary condition can be applied easily and directly without any additional numerical effort. Compared with IMLS method presented by Lancaster and Salkauskas, the IIMLS method uses the nonsingular weight function. Then the IIMLS method can overcome the difficulty caused by the singularity of the weight function in the IMLS method. Any weight function used in the MLS approximation can be chosen as the weight function of the IIMLS method. And the number of unknown coefficients in the trial function of the IIMLS method is less than that of the MLS approximation. Hence, the IIEFG method gives high computational precision.

## References


[1] Liu Z S, Harsono E and Swaddiwudhipong S 2009 *Int. J. Appl. Mech.* **1** 61

[2] Liu Z S, Hong W, Suo Z G, Swaddiwudhipong S and Zhang Y W 2010 *Comput. Mater. Sci.* **49** 60

[3] Brebbia C A and Wrobel L C 1984 *Boundary Element Techniques: Theory and Applications in Engineering* (Berlin: Springer-Verlag)

[4] Chen S S, Li Q and Liu Y 2012 *Chin. Phys. B* **21** 110207

[5] Cheng R J and Ge H X 2012 *Chin. Phys. B* **21** 100209

[6] Cheng Y M and Peng M J 2005 *Sci. China Ser. G: Phys. Mech. Astron.* **48** 641

[7] Yang X L, Dai B D and Zhang W W 2012 *Chin. Phys. B* **21** 100208

[8] Cheng Y M, Li R X and Peng M J 2012 *Chin. Phys. B* **21** 090205

[9] Belytschko T, Lu Y Y and Gu L 1994 *Int. J. Numer. Meth. Eng.* **37** 229

[10] Liu W K, Jun S and Zhang Y F 1995 *Int. J. Numer. Meth. Eng.* **20** 1081

[11] Liu G R and Gu Y T 2004 *Eng. Anal. Bound. Elem.* **28** 475

[12] Zhang J M and Tanaka M 2004 *Int. J. Numer. Meth. Eng.* **41** 1147

[13] Zhang J M and Tanaka M 2008 *Comput. Mech.* **41** 777

[14] Bai F N, Li D M, Wang J F and Cheng Y M 2012 *Chin. Phys. B* **21** 020204

[15] Liew K M, Ren J and Reddy J N 2005 *Int. J. Numer. Meth. Eng.* **63** 1014

[16] Shepard D 1968 *Proceeding of the 23rd ACM National Conference* (New York) p. 517

[17] Lancaster P and Salkauskas K 2007 *Math. Comput.* **37** 141

[18] Kaljevic I and Saigal S 1997 *Int. J. Numer. Meth. Eng.* **40** 2953

[19] Ren H P, Cheng Y M and Zhang W 2009 *Chin. Phys. B* **18** 4065

[20] Ren H P, Cheng Y M and Zhang W 2010 *Sci. China Ser. G: Phys. Mech. Astron.* **53** 758

[21] Ren H Pand Cheng Y M 2011 *Int. J. Appl. Mech.* **3** 735

[22] Ren H P and Cheng Y M 2012 *Eng. Anal. Bound. Elem.* **36** 873

[23] Netuzhylov H 2008 *Eng. Anal. Bound. Elem.* **32** 512

[24] Thomas M and Christian B 2008 *Eng. Anal. Bound. Elem.* **32** 461

[25] Wang J F, Sun F X and Cheng Y M 2012 *Chin. Phys. B* **21** 090204

[26] Timoshenko S P and Goodier J N 1970 *Theory of Elasticity*, 3rd edn. (New York: McGraw-Hill)

[27] Liu G R and Gu Y T 2001 *Int. J. Numer. Meth. Eng.* **50** 937